ISSN 0915-633X

NATIONAL INSTITUTE FOR FUSION SCIENCE

Comparison of Multichain Coulomb Polymers in Isolated and Periodic Systems: Molecular Dynamics Study

M. Tanaka, A. Yu Grosberg and T. Tanaka

(Received - Dec. 24, 1998)

NIFS-581 Jan. 1999

RESEARCH REPORT
NIFS Series

NAGOYA, JAPAN

Comparison of Multichain Coulomb Polymers in Isolated and Periodic Systems: Molecular Dynamics Study

Motohiko Tanaka[1], A.Yu Grosberg[2,3], and Toyoichi Tanaka[2]

[1] *National Institute for Fusion Science, Oroshi-cho, Toki 509-5292, Japan*
[2] *Massachusetts Institute of Technology, Cambridge, Massachusetts 02139, USA*
[3] *Institute of Biochemical Physics, Russian Academy Sci., Moscow 117977, Russia*

Abstract

The effects of periodic boundary conditions are examined for multichain Coulomb polymers that are composed of both positively and negatively-charged monomers (polyampholyte). At high temperature, polyampholyte takes a large volume with its chains spreading homogeneously in the whole domain. At low temperature where the Coulomb energy prevails over the thermal energy, the polyampholyte is collapsed to form a globule. The resultant globule is somewhat more compressed than that in an isolated (wall-bound) system. The effect of added salt is also mentioned briefly.

Keywords: molecular dynamics, periodic boundary conditions, the Ewald's sum, multichain polyampholyte, strongly-coupled Coulomb system, salt electrolyte solution.

1. Introduction

Electrically charged polymers that are widely found in daily products and live organisms like DNA and RNA constitute a many-body Coulomb system, which is electrostatically strongly-coupled even at room temperature due to predominance of the Coulomb energy over the kinetic (thermal) energy, $e^2/\epsilon aT \geq 1$. Such polymers are categorized to *polyelectrolytes* and *polyampholytes*. The former polymers are composed of monomers of one charge sign, and the latter polymers contain both positive and negative monomers which enable them self-neutralization. These polymers are known to be highly controlled by co-existing counter-ions or added salt ions through electrostatic shielding. Also, the Coulomb attraction force let the polymers form a network of chains either above certain concentration or below some temperature.

The properties of charged polymers, both for polyelectrolyte and polyampholyte regimes, were studied extensively by a series of experimental[1] and theoretical[2,3] works and numerical[4,5] studies. The charged polymers that we are going to study here consist of both positively and negatively charged monomers, with their sequence along the chains being at random. This kind of charged polymers is called *quenched* polyampholyte, since its sequence and properties are deter-

mined by the synthesis chemistry. In this paper, we first summarize the results of single-chain polyampholytes[5], where occurrence of highly collapsed globule and a hysteresis are proven numerically. Then, we present a dynamical process and the structure formation associated with multichain polyampholytes under the periodic boundary conditions. We adopt the Ewald's PME method[6,7] to take infinite sums over the true and image charges for the long-range Coulomb force. In the final part of this paper, we show the effect of added salt on polyampholytes[8].

2. Equations of Motion

In molecular dynamics (MD) simulations, a system of charged polymers is described by a set of *Langevin-type* equations of motion,

$$m d\mathbf{v}_i/dt = \mathbf{F}_{LR}(\mathbf{r}_i) - (3T/a^2)(2\mathbf{r}_i - \mathbf{r}_{i+1} - \mathbf{r}_{i-1}) + \mathbf{F}_{th} - \nu m \mathbf{v}_i, \quad (1)$$

$$d\mathbf{r}_i/dt = \mathbf{v}_i, \quad (2)$$

where $\mathbf{r}_i$ and $\mathbf{v}_i$ are the position and velocity of the i-th monomer ($i = 1 \sim N$), respectively, and $\mathbf{F}_{th}$ is random thermal force and ν the friction constant. The long-range Coulomb force $\mathbf{F}_{LR}$ is obtained by direct summation over possible monomer pairs,

$$\mathbf{F}_{LR}(\mathbf{r}_i) = \sum_{j=1}^{N}{}' Z_i Z_j e^2 \hat{\mathbf{r}}_{ij}/\epsilon|\mathbf{r}_i - \mathbf{r}_j|^2, \quad (3)$$

where $\hat{\mathbf{r}}_{ij}$ is a unit vector along $(\mathbf{r}_i - \mathbf{r}_j)$, ϵ the electric permitivity, and $(')$ means omission of $j = i$ in the summation. For the isolated polyampholytes, the summation of Eq.(3) is made only for the true charges in the primary domain. Eqs.(1),(2) are time integrated under the boundary condition of a reflecting wall.

3. The Ewald's Sum: Periodic System

For the study of continuous polyampholyte medium, we use the periodic boundary conditions, where the summation of Eq.(3) should be replaced by that over the true and image charges[6,7],

$$\mathbf{F}_{LR}^{(P)}(\mathbf{r}_i) = \sum_{j=1}^{N} \sum_{\mathbf{n}\in\mathbf{Z}}{}' Z_i Z_j e^2 \tilde{\mathbf{R}}_{ij}/\epsilon|\mathbf{R}_{ij}|^2, \quad (4)$$

where $\mathbf{R}_{ij} = \mathbf{r}_i - \mathbf{r}_j + \mathbf{n}L$, $\tilde{\mathbf{R}}_{ij}$ is a unit vector along $\mathbf{R}_{ij}$, L the side length of periodicity, and $\mathbf{n}$ a three-dimensional integer vector. To avoid difficulties of infinite sums over $\mathbf{n}$, the Ewald method is used which splits the inverse-distance term into the rapidly changing short-range part and the smooth long-range part as,

$$1/r = f(r)/r + (1 - f(r))/r, \quad (5)$$

where $f(r)$ is a smooth function that vanishes at large distances. With the choice of the complementary error function for $f(r)$, $\mathrm{erfc}(r) = 2\pi^{-1/2}\int_r^\infty \exp(-t^2)dt$, the sum in Eq.(4) that corresponds to the second term of Eq.(5) gives rise to the electrostatic potential $\tilde{\Phi}(\mathbf{k}) = (4\pi/k^2)\exp(-k^2/4\alpha^2)\tilde{\rho}(\mathbf{k})$ in the Fourier space. Here, $\tilde{\rho}(\mathbf{k})$ is a Fourier-transformed charge density, and α is an arbitrary parameter that sensitively affects accuracy of the sums for chosen real and Fourier space cutoffs, r_{max} and k_{max}. This potential is calculated efficiently with the use of the fast Fourier transform (FFT); the force due to this contribution is derived from the back Fourier-transformed potential $\Phi(\mathbf{r})$ by $\mathbf{F}^{(k)}(\mathbf{r}) = -q_i\nabla\Phi(\mathbf{r})$. The direct sum in Eq.(4) due to the first term of Eq.(5) is given by,

$$\mathbf{F}_i^{(r)} = q_i \sum_{j=1}^{N} \sum_{\mathbf{n}\in\mathbf{Z}}{}' \left(\frac{2\alpha}{\sqrt{\pi}} \exp(-\alpha^2 R_{ij}^2)/R_{ij} \right.$$

$$+\mathrm{erfc}(\alpha R_{ij})/R_{ij}^2\Big)\,\hat{\mathbf{R}}_{ij}. \qquad (6)$$

A suitable choice of the Ewald parameter α and summation cutoffs, and the charge and field interpolation schemes are found in the previous literatures[6,7].

4. Single-Chain Polyampholytes

The first non-lattice type simulation for single-chain polyampholytes with the use of molecular dynamics simulation[5] showed that:
(1) Folding of the chain occurs in a time scale of 100 ps. The equilibrium conformation is a globule if charge imbalance of monomers is less than $\sqrt{N}$, and that it is a stretched Gaussian coil for highly charged case, where N is the number of monomers (Figure 1).
(2) Three temperature regimes are identified for the gyration radius, i.e., the structure of polyampholytes, which are the globular, transition, and stretched coil regimes at low, medium, and high temperatures, respectively (Figure 2). The globule at low temperature is due to intensive folding of the chain, which is much more compact than that obtained by lattice-type simulations[4].
(3) Cooperation of the short-range attraction force and the long-range Coulomb force gives rise to a hysteresis in the volume of polyampholyte against a slow cyclic change of temperature (Figure 3).

These are the results corresponding to experiments of very low density solution of polyampholyte, or those with an extracted single-chain of the DNA coil.

5. Multichain Polyampholytes (Periodic)

(a) Dynamical behaviors

Multichain polyampholytes have more freedom to expand compared to single-chain ones, since the chains are not connected. At high temperature, the volume that polyampholyte chains occupy is bound only by the container size, since diffusion proceeds infinitely due to thermal agitations.

The time history of the kinetic energy W_{kin}, electrostatic energy Φ_{ES}, and elastic energy W_{spr} per monomer is shown for high temperature $T/T_0 = 1$ ($R_{max} = 42a$) on the left column of Figure 4 (T_0 is the base temperature defined by $e^2/\epsilon a T_0 = 1$). That of the gyration radius of the whole polyampholyte $R_{g,sys}$, the gyration radius of a specific chain R_{g1}, and the x-component velocity of a monomer is shown on the right column. Energy equi-partition holds between the kinetic and elastic energies. The expansion speed of the chains is deduced to be about 20% that of the thermal speed $v_{th} = (3/4\pi\Gamma)^{1/2} a\omega_p$ ($\Gamma = T_0/T$),

$$V_{diff} = dR_{g,sys}/dt \sim 0.1 a\omega_p \sim 0.2 v_{th}, \quad (7)$$

Large time fluctuations in the gyration radius reveal undamped folding /unfolding oscillations of the chains in a viscous Langevin fluid. Each monomer is also under thermal vibrations as seen in V_x.

Figure 5 shows the typical conformations that the randomly co-polymerized multichain polyampholytes take at (a) high temperature $T/T_0 = 1$, and (b) low temperatures $T/T_0 = 1/8$. At high temperature, the chains tend to distribute homogeneously in the domain, but their relative positions are quite variable in time due to thermal fluctuations. On the other hand, a stable and compact globule conformation is taken in each domain at low temperature. Although the monomers

are under thermal vibrations, the radius of the globule is almost constant in time.

(b) Statistical Properties

The temperature dependence of the polyampholyte is shown in Figure 6; the system gyration radius $R_{g,sys}$, the average of gyration radii of the chains R_{g1}, and the filling index $\zeta = N_c^{1/3} R_{g1}/R_{g,sys}$ are displayed for six 32-mer polyampholytes, where N_c is a number of chains that make up the polyampholyte. (Each data point is an average over ten independent runs.) The side length of the simulation box (or the periodicity length) is $R_{max} = 42a$. Both the gyration radii $R_{g,sys}$ and R_{g1} are increasing functions of temperature. However, for the multichain polyampholyte at high temperature, the radius of the system (whole chains) increases much faster than that of each chain R_{g1}, since the chains are not connected. The system gyration radius is only limited by the container size or periodicity. The polyampholyte swells infinitely under non-bound (unconfined) boundary conditions[8]. By the filling index, we can measure the degree of chain entanglement (overlapping). The condition $\zeta \geq 1$ means that the chains are well overlapped, which is achieved at low temperature $T/T_0 < 0.2$.

Also in Figure 6, a comparison of different boundary conditions is made, where "Isolated" corresponds to the run with a reflecting boundary condition, and "Periodic" to those with periodic boundary conditions. Both kind of gyration radii, $R_{g,sys}$ and R_{g1} are smaller in the periodic system at low temperature, which tells occurrence of more compression in the continuous medium. However, at high temperature the chains are more homogeneously distributed in the periodic system; the chains tend to stay away from the boundary wall in the isolated system.

The effect of the domain size is shown in Figure 7. The difference occurs only at high temperature $T/T_0 > 0.5$, for which the typical state of the polyampholyte is a wall-bound one that consists of separate chains. The ratio of the gyration radii for the cases with $R_{max} = 42$ and 28 is exactly the ratio of the domain size, $42/28 = 1.5$. At low temperature, little difference is found since a compact globule that is the typical state the chains is not affected by the domain volume.

Detailed MD simulation results of multichain polyampholytes, including the effect of charge sequences, stiffness, the molecular weight and the number of the chains, the formation and stability of the globular state, under the wall boundary condition are described in a separate publication[8].

6. The Effects of Added Salt

As salt causes swelling of charged gels, an addition of salt on polyampholyte makes the globule loose and soluble to solvent. In the MD simulation below[8], salt ions are placed homogeneously at the beginning of the run, where the charge density of salt ions is comparable to that of the polyampholyte in a globule.

Figure 8 shows the system gyration radius $R_{g,sys}$, average of gyration radii R_{g1}, and the filling index ζ for the polyampholytes in salt aqueous solution (open circle) and in salt-free solvent (solid circle). As shown, the gyration radius of polyampholyte increases if salt is added. This is more apparent at low temper-

ature where a compact globule is the typical state of the chains in the salt-free solvent. A scatter plot of the polyampholyte clearly tells us that the globule becomes loose with its surface fuzzy and irregular after addition of salt. The time evolution of disintegration process of the globule is described in a separate publication[8].

Acknowledgments

One of the authors (M.T.) would like to thank Dr.K.Kremer and Dr.C.Holm for discussions of the Ewald's sum method for polymer systems.

References

1. References in F.Candau and J.F.Joanny, *Encyclopedia of Polymeric Materials, 7*, 5476 (edited by J.C.Salomone, CRC Press, Boca Raton, 1996).
2. A.V.Dobrynin and M.Rubinstein, *J.de Phys.II, 5*, 677 (1995).
3. R.Everaers, A.Johner, and J.-F.Joanny, *Macromolecules, 30*, 8478 (1997).
4. Y.Kantor, M.Kardar and H.Li, *Phys.Review, E49*, 1383 (1994).
5. M.Tanaka, A.Yu Grosberg, V.S.Pande, and T.Tanaka, *Phys.Review, E56*, 5798 (1997).
6. H.Petersen, *J.Chem.Phys., 103*, 3668 (1995).
7. M.Deserno and C.Holm, *How to mesh up Ewald sums (in press)* (1998).
8. M.Tanaka, A.Yu Grosberg, and T.Tanaka, *NIFS Report No.579; submitted to J.Chem.Phys.* (1998).

Figure Captions

Figure 1.: Non-neutral charge effect: (a) almost neutral case, $\delta N/N = 1.6\%$, (b) 6.3%, (c) highly charged case, 14.1%.

Figure 2.: The temperature dependence of the gyration radius for neutral polyampholytes of 64, 128 and 256 mers.

Figure 3.: A hysteresis of the gyration radius of polyampholyte against slow cyclic change of temperature, obtained for a single 64-mer.

Figure 4.: The time history of the kinetic energy W_{kin}, electrostatic energy Φ_{ES}, elastic energy W_{spr} on the left column, and that of the system (whole polyampholyte) $R_{g,sys}$, the gyration radius of a chain, and the velocity of a monomer.

Figure 5.: The typical conformations that the polyampholyte chains take at (a) high temperature $T/T_0 = 1$, and (b) low temperature $T/T_0 = 1/8$. Two consecutive domains in the x-direction are displayed.

Figure 6.: The effect of different boundary conditions is seen between the wall-bound and periodic systems.

Figure 7.: The effect of domain size under the periodic boundary conditions is shown for $R_{max} = 28$ and 42 cases.

Figure 8.: The effect of added salt is shown for randomly co-polymerized six 32-mer polyampholyte. Results for the salt-free case are also shown.

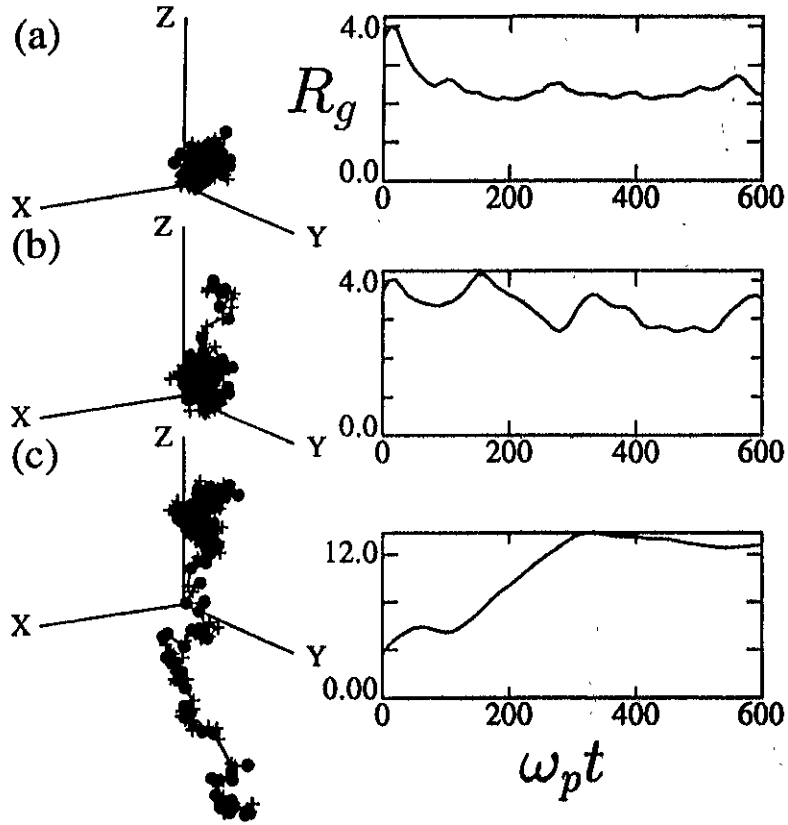
(a)
Z
X
Y
(b)
Z
X
Y
(c)
Z
X
Y
R_g
4.0
0.0
0
200
400
600
4.0
0.0
0
200
400
600
12.0
0.00
0
200
400
600
$\omega_p t$

Fig. 1

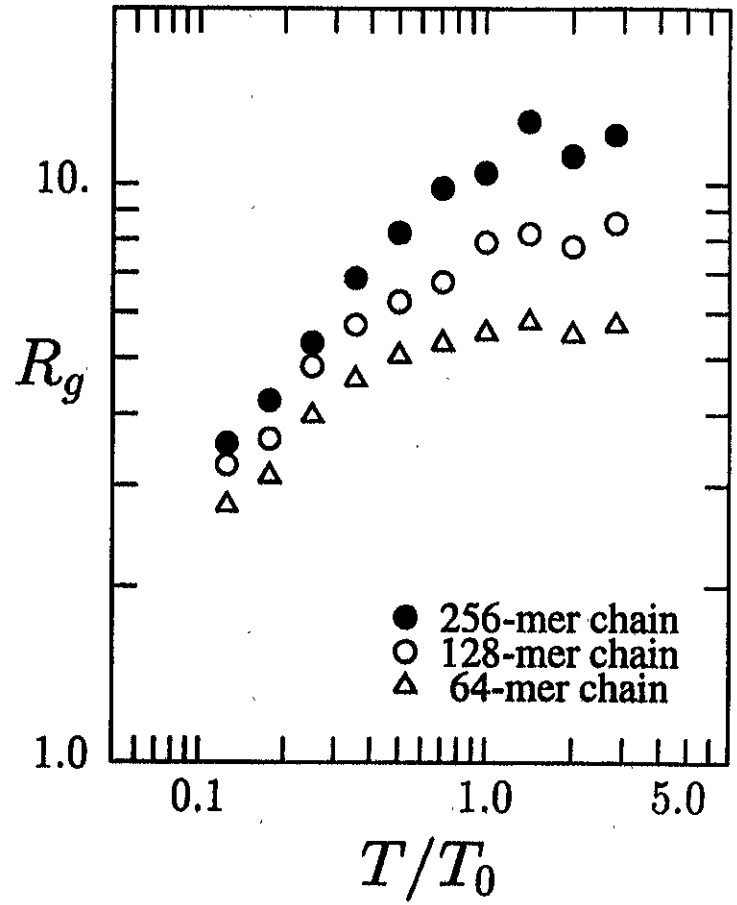
10.
1.0
R_g
0.1
1.0
5.0
T/T_0
256-mer chain
128-mer chain
64-mer chain

Fig. 2

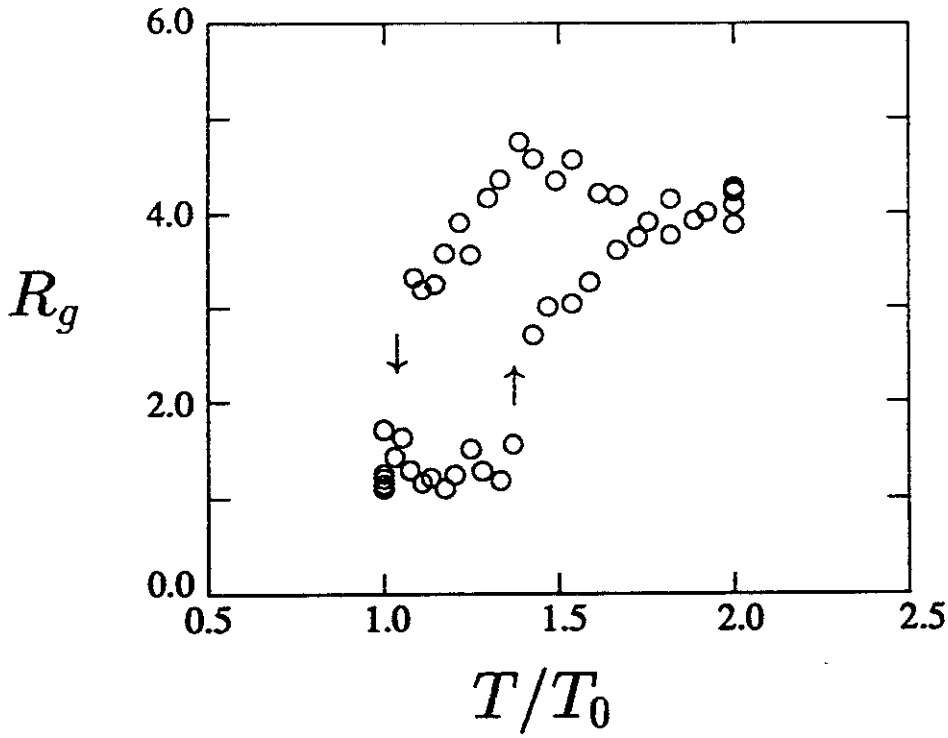
6.0
4.0
2.0
0.0
R_g
0.5
1.0
1.5
2.0
2.5
T/T_0

Fig. 3

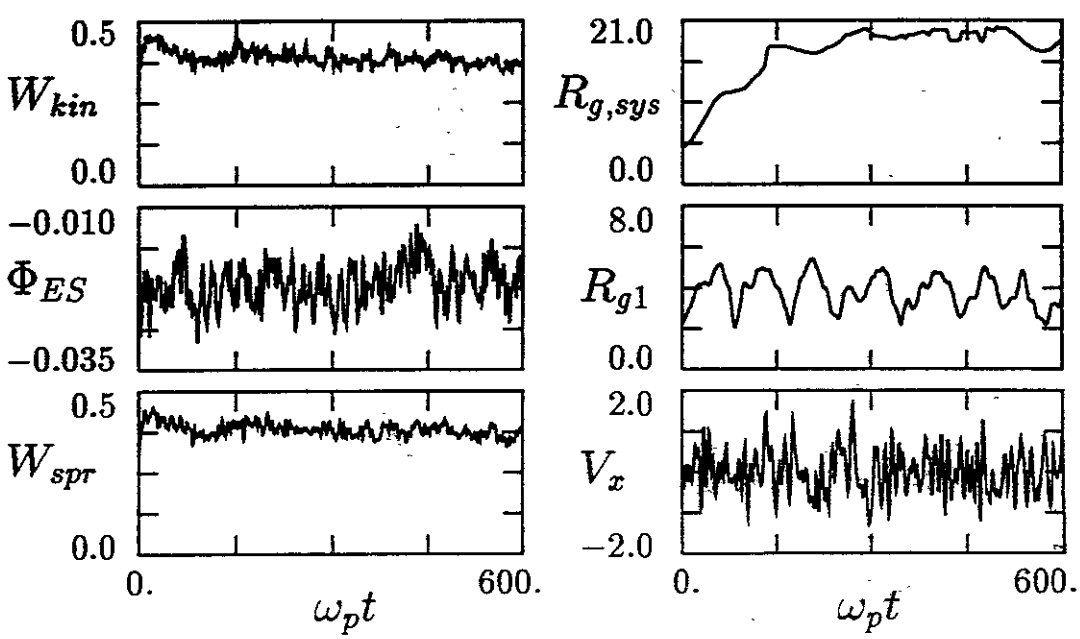
0.5
W_{kin}
0.0
−0.010
Φ_{ES}
−0.035
0.5
W_{spr}
0.0
0.
600.
$\omega_p t$
21.0
$R_{g,sys}$
0.0
8.0
R_{g1}
0.0
2.0
V_x
−2.0
0.
600.
$\omega_p t$

Fig. 4

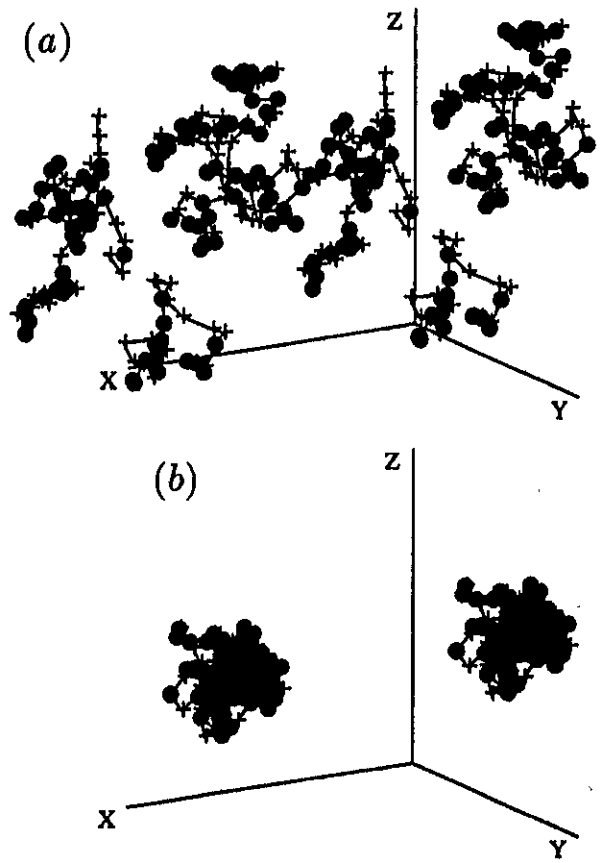
(a)
Z
X
Y
(b)
Z
X
Y

Fig. 5

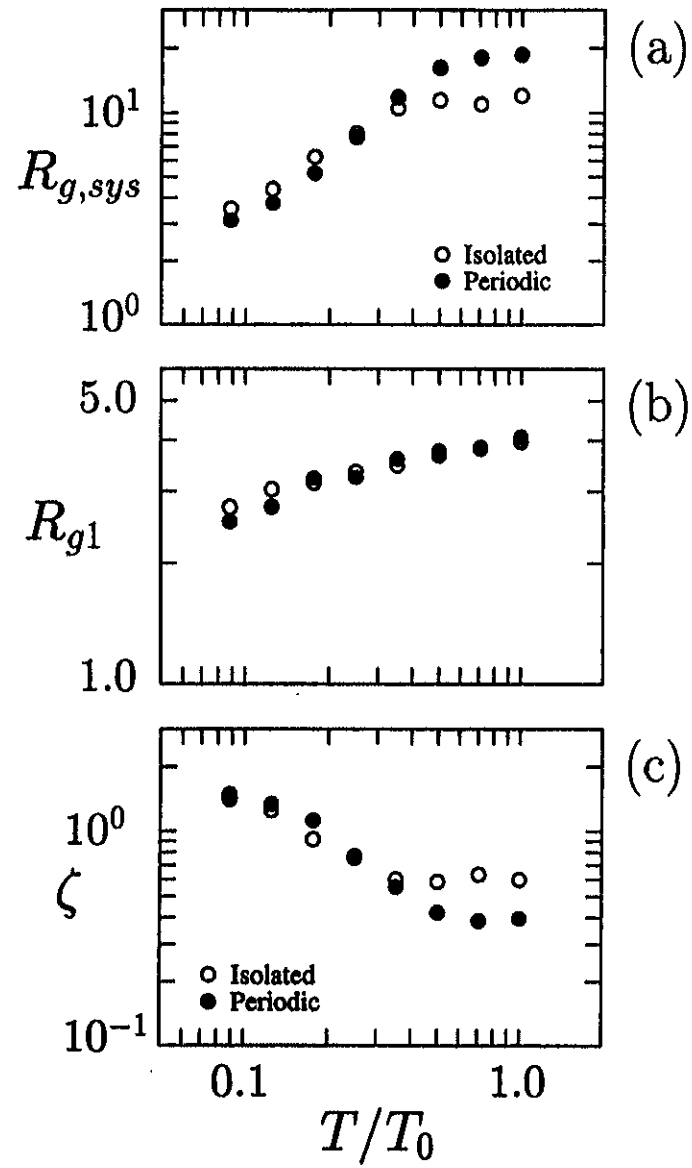
(a)
10^1
$R_{g,sys}$
Isolated
Periodic
10^0
5.0
(b)
R_{g1}
1.0
(c)
10^0
ζ
Isolated
Periodic
10^{-1}
0.1
1.0
T/T_0

Fig. 6

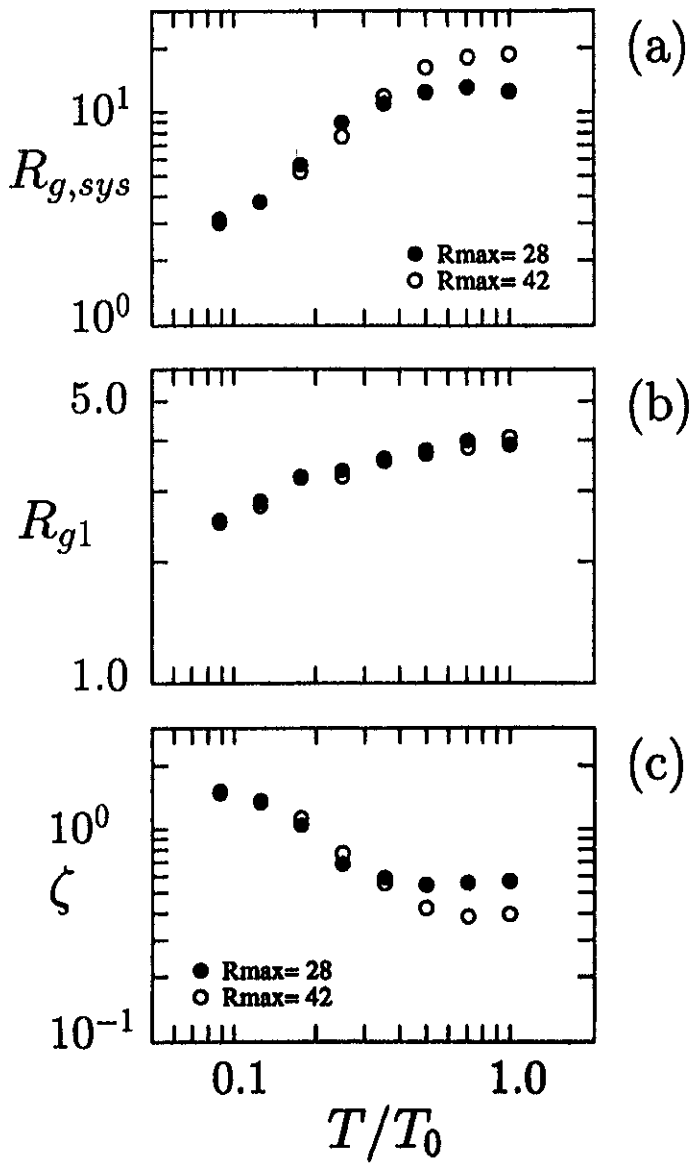
(a)
10^1
$R_{g,sys}$
10^0
Rmax= 28
Rmax= 42
(b)
5.0
R_{g1}
1.0
(c)
10^0
ζ
10^{-1}
Rmax= 28
Rmax= 42
0.1
1.0
T/T_0

Fig. 7

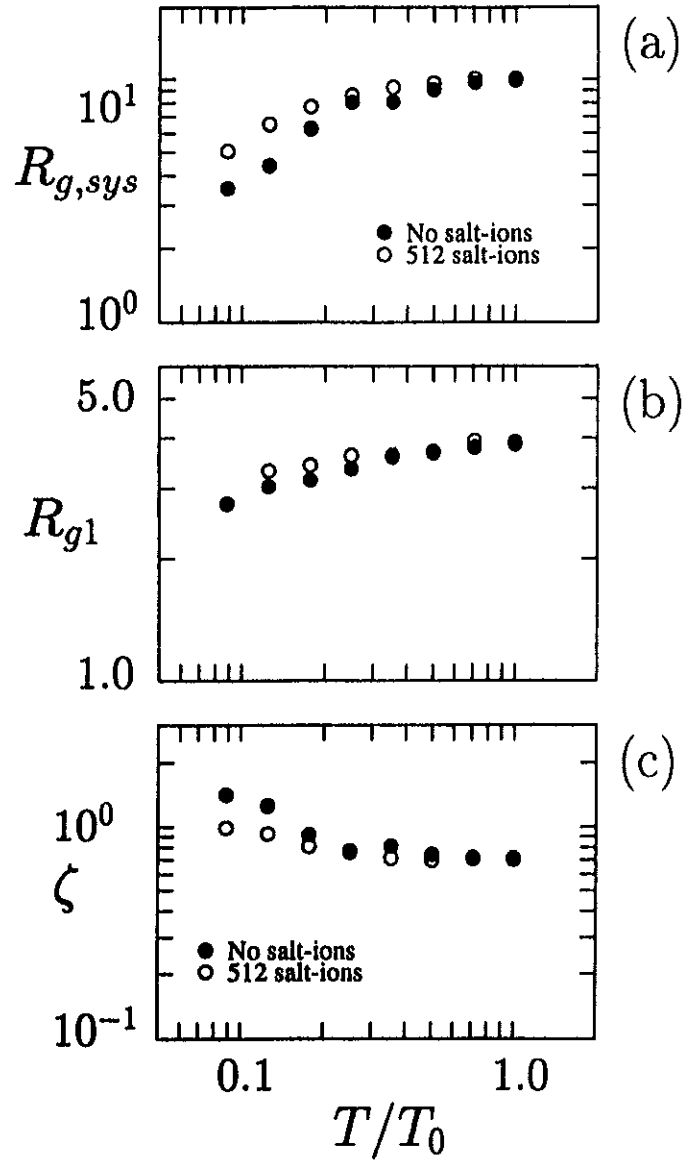
(a)
10^1
$R_{g,sys}$
10^0
No salt-ions
512 salt-ions
(b)
5.0
R_{g1}
1.0
(c)
10^0
ζ
10^{-1}
No salt-ions
512 salt-ions
0.1
1.0
T/T_0

Fig. 8

Recent Issues of NIFS Series

NIFS-517 John L. Johnson,
The Quest for Fusion Energy; Oct 1997

NIFS-518 J. Chen, N Nakajima and M. Okamoto,
Shift-and-Inverse Lanczos Algorithm for Ideal MHD Stability Analysis; Nov. 1997

NIFS-519 M. Yokoyama, N. Nakajima and M. Okamoto,
Nonlinear Incompressible Poloidal Viscosity in L=2 Heliotron and Quasi-Symmetric Stellarators, Nov. 1997

NIFS-520 S. Kida and H. Miura,
Identificaiton and Analysis of Vortical Structures; Nov. 1997

NIFS-521 K. Ida, S Nishimura, T. Minami, K. Tanaka, S. Okamura, M Osakabe, H Idei, S. Kubo, C. Takahashi and K. Matsuoka,
High Ion Temperature Mode in CHS Heliotron/torsatron Plasmas; Nov. 1997

NIFS-522 M. Yokoyama, N. Nakajima and M. Okamoto,
Realization and Classification of Symmetric Stellarator Configurations through Plasma Boundary Modulations; Dec. 1997

NIFS-523 H. Kitauchi,
Topological Structure of Magnetic Flux Lines Generated by Thermal Convection in a Rotating Spherical Shell; Dec. 1997

NIFS-524 T. Ohkawa,
Tunneling Electron Trap; Dec. 1997

NIFS-525 K. Itoh, S.-I. Itoh, M. Yagi, A. Fukuyama,
Solitary Radial Electric Field Structure in Tokamak Plasmas; Dec. 1997

NIFS-526 Andrey N. Lyakhov,
Alfven Instabilities in FRC Plasma; Dec. 1997

NIFS-527 J. Uramoto,
Net Current Increment of negative Muonlike Particle Produced by the Electron and Positive Ion Bunch-method; Dec. 1997

NIFS-528 Andrey N. Lyakhov,
Comments on Electrostastic Drift Instabilities in Field Reversed Configuraiton; Dec. 1997

NIFS-529 J. Uramoto,
Pair Creation of Negative and Positive Pionlike (Muonlike) Particle by Interaction between an Electron Bunch and a Positive Ion Bunch; Dec. 1997

NIFS-530 J. Uramoto,
Measuring Method of Decay Time of Negative Muonlike Particle by Beam Collector Applied RF Bias Voltage; Dec. 1997

NIFS-531 J. Uramoto,
Confirmation Method for Metal Plate Penetration of Low Energy Negative Pionlike or Muonlike Particle Beam under Positive Ions; Dec. 1997

NIFS-532 J. Uramoto,
Pair Creations of Negative and Positive Pionlike (Muonlike) Particle or K Mesonlike (Muonlike) Particle in H2 or D2 Gas Discharge in Magnetic Field; Dec. 1997

NIFS-533 S. Kawata, C. Boonmee, T. Teramoto, L. Drska, J. Limpouch, R. Liska, M Sinor,
Computer-Assisted Particle-in-Cell Code Development; Dec 1997

NIFS-534 Y Matsukawa, T. Suda, S. Ohnuki and C. Namba,
Microstructure and Mechanical Property of Neutron Irradiated TiNi Shape Memory Alloy, Jan 1998

NIFS-535 A. Fujisawa, H Iguchi, H. Idei, S. Kubo, K Matsuoka, S. Okamura, K Tanaka, T Minami, S Ohdachi, S Morita, H Zushi, S Lee,

M. Osakabe, R. Akiyama, Y. Yoshimura, K. Toi, H. Sanuki, K. Itoh, A. Shimizu, S. Takagi, A. Ejiri, C. Takahashi, M. Kojima, S. Hidekuma, K. Ida, S. Nishimura, N. Inoue, R. Sakamoto, S.-I. Itoh, Y. Hamada, M. Fujiwara,
Discovery of Electric Pulsation in a Toroidal Helical Plasma; Jan. 1998

NIFS-536 Lj.R. Hadzievski, M.M. Skoric, M. Kono and T. Sato,
Simulation of Weak and Strong Langmuir Collapse Regimes; Jan. 1998

NIFS-537 H. Sugama, W. Horton,
Nonlinear Electromagnetic Gyrokinetic Equation for Plasmas with Large Mean Flows; Feb. 1998

NIFS-538 H. Iguchi, T.P. Crowley, A. Fujisawa, S. Lee, K. Tanaka, T. Minami, S. Nishimura, K. Ida, R. Akiyama, Y. Hamada, H., Idei. M. Isobe, M. Kojima, S. Kubo, S. Morita, S. Ohdachi, S. Okamura, M. Osakabe, K. Matsuoka, C. Takahashi and K. Toi,
Space Potential Fluctuations during MHD Activities in the Compact Helical System (CHS); Feb. 1998

NIFS-539 Takashi Yabe and Yan Zhang,
Effect of Ambient Gas on Three-Dimensional Breakup in Coronet Formation Process; Feb. 1998

NIFS-540 H. Nakamura, K. Ikeda and S. Yamaguchi,
Transport Coefficients of InSb in a Strong Magnetic Field; Feb. 1998

NIFS-541 J. Uramoto,
Development of ν_μ Beam Detector and Large Area ν_μ Beam Source by H_2 Gas Discharge (I); Mar. 1998

NIFS-542 J. Uramoto,
Development of $bar{\nu}_\mu$ Beam Detector and Large Area $bar{\nu}_\mu$ Beam Source by H_2 Gas Discharge (II); Mar. 1998

NIFS-543 J. Uramoto,
Some Problems inside a Mass Analyzer for Pions Extracted from a H_2 Gas Discharge; Mar. 1998

NIFS-544 J. Uramoto,
Simplified ν_μ $bar{\nu}_\mu$ Beam Detector and ν_μ $bar{\nu}_\mu$ Beam Source by Interaction between an Electron Bunch and a Positive Ion Bunch; Mar. 1998

NIFS-545 J. Uramoto,
Various Neutrino Beams Generated by D_2 Gas Discharge; Mar.1998

NIFS-546 R. Kanno, N. Nakajima, T. Hayashi and M. Okamoto,
Computational Study of Three Dimensional Equilibria with the Bootstrap Current; Mar. 1998

NIFS-547 R. Kanno, N. Nakajima and M. Okamoto,
Electron Heat Transport in a Self-Similar Structure of Magnetic Islands; Apr. 1998

NIFS-548 J.E. Rice,
Simulated Impurity Transport in LHD from MIST; May 1998

NIFS-549 M.M. Skoric, T. Sato, A.M. Maluckov and M.S. Jovanovic,
On Kinetic Complexity in a Three-Wave Interaction; June 1998

NIFS-550 S. Goto and S. Kida,
Passive Saclar Spectrum in Isotropic Turbulence: Prediction by the Lagrangian Direct-interaction Approximation; June 1998

NIFS-551 T. Kuroda, H. Sugama, R. Kanno, M. Okamoto and W. Horton,
Initial Value Problem of the Toroidal Ion Temperature Gradient Mode ; June 1998

NIFS-552 T. Mutoh, R. Kumazawa, T. Seki, F. Simpo, G. Nomura, T. Ido and T. Watari,
Steady State Tests of High Voltage Ceramic Feedthoughs and Co-Axial Transmission Line of ICRF Heating System for the Large Helical Device ; June 1998

NIFS-553 N. Noda, K. Tsuzuki, A. Sagara, N. Inoue, T. Muroga,
oronaization in Future Devices -Protecting Layer against Tritium and Energetic Neutrals-: July 1998

NIFS-554 S. Murakami and H Saleem,
Electromagnetic Effects on Rippling Instability and Tokamak Edge Fluctuations, July 1998

NIFS-555 H. Nakamura , K. Ikeda and S. Yamaguchi,
Physical Model of Nernst Element; Aug 1998

NIFS-556 H. Okumura, S. Yamaguchi, H. Nakamura, K. Ikeda and K. Sawada,
Numerical Computation of Thermoelectric and Thermomagnetic Effects; Aug. 1998

NIFS-557 Y. Takeiri, M. Osakabe, K. Tsumori, Y Oka, O. Kaneko, E. Asano, T. Kawamoto, R. Akiyama and M. Tanaka,
Development of a High-Current Hydrogen-Negative Ion Source for LHD-NBI System; Aug.1998

NIFS-558 M. Tanaka, A. Yu Grosberg and T Tanaka,
Molecular Dynamics of Structure Organization of Polyampholytes; Sep. 1998

NIFS-559 R. Horiuchi, K. Nishimura and T. Watanabe,
Kinetic Stabilization of Tilt Disruption in Field-Reversed Configurations; Sep. 1998
(IAEA-CN-69/THP1/11)

NIFS-560 S. Sudo, K. Kholopenkov, K. Matsuoka, S. Okamura, C. Takahashi, R. Akiyama, A. Fujisawa, K. Ida, H. Idei, H. Iguchi, M. Isobe, S. Kado, K. Kondo, S. Kubo, H. Kuramoto, T. Minami, S. Morita, S. Nishimura, M. Osakabe, M. Sasao, B Peterson, K Tanaka, K. Toi and Y. Yoshimura,
Particle Transport Study with Tracer-Encapsulated Solid Pellet Injection; Oct. 1998
(IAEA-CN-69/EXP1/18)

NIFS-561 A. Fujisawa, H. Iguchi, S. Lee, K. Tanaka, T. Minami, Y. Yoshimura, M. Osakabe, K. Matsuoka, S. Okamura, H. Idei, S. Kubo, S. Ohdachi, S. Morita, R. Akiyama, K. Toi, H. Sanuki, K. Itoh, K. Ida, A. Shimizu, S. Takagi, C. Takahashi, M. Kojima, S. Hidekuma, S. Nishimura, M. Isobe, A. Ejiri, N. Inoue, R. Sakamoto, Y. Hamada and M. Fujiwara,
Dynamic Behavior Associated with Electric Field Transitions in CHS Heliotron/Torsatron; Oct. 1998
(IAEA-CN-69/EX5/1)

NIFS-562 S. Yoshikawa,
Next Generation Toroidal Devices; Oct. 1998

NIFS-563 Y. Todo and T. Sato,
Kinetic-Magnetohydrodynamic Simulation Study of Fast Ions and Toroidal Alfvén Eigenmodes; Oct. 1998
(IAEA-CN-69/THP2/22)

NIFS-564 T. Watari, T. Shimozuma, Y. Takeiri, R. Kumazawa, T. Mutoh, M. Sato, O. Kaneko, K. Ohkubo, S. Kubo, H. Idei, Y. Oka, M. Osakabe, T. Seki, K. Tsumori, Y. Yoshimura, R. Akiyama, T. Kawamoto, S. Kobayashi, F. Shimpo, Y. Takita, E. Asano, S. Itoh, G. Nomura, T. Ido, M. Hamabe, M. Fujiwara, A. Iiyoshi, S. Morimoto, T. Bigelow and Y.P. Zhao,
Steady State Heating Technology Development for LHD; Oct. 1998
(IAEA-CN-69/FTP/21)

NIFS-565 A. Sagara, K.Y. Watanabe, K. Yamazaki, O. Motojima, M. Fujiwara, O. Mitarai, S Imagawa, H. Yamanishi, H. Chikaraishi, A. Kohyama, H. Matsui, T. Muroga, T. Noda, N. Ohyabu, T. Satow, A.A. Shishkin, S. Tanaka, T. Terai and T. Uda,
LHD-Type Compact Helical Reactors; Oct. 1998
(IAEA-CN-69/FTP/03(R)

NIFS-566 N. Nakajima, J. Chen, K. Ichiguchi and M. Okamoto,
Global Mode Analysis of Ideal MHD Modes in L=2 Heliotron/Torsatron Systems; Oct. 1998
(IAEA-CN-69/THP1/08)

NIFS-567 K. Ida, M. Osakabe, K. Tanaka, T. Minami, S. Nishimura, S. Okamura, A. Fujisawa, Y. Yoshimura, S. Kubo, R. Akiyama, D.S.Darrow, H. Idei, H. Iguchi, M. Isobe, S. Kado, T. Kondo, S. Lee, K. Matsuoka, S. Morita, I. Nomura, S. Ohdachi, M. Sasao, A. Shimizu, K. Tumori, S. Takayama, M. Takechi, S. Takagi, C. Takahashi, K. Toi and T. Watari,
Transition from L Mode to High Ion Temperature Mode in CHS Heliotron/Torsatron Plasmas; Oct. 1998
(IAEA-CN-69/EX2/2)

NIFS-568 S. Okamura, K. Matsuoka, R. Akiyama, D.S. Darrow, A. Ejiri, A. Fujisawa, M. Fujiwara, M. Goto, K. Ida H. Idei, H. Iguchi, N. Inoue, M. Isobe, K. Itoh, S. Kado, K. Khlopenkov, T. Kondo, S. Kubo, A. Lazaros, S Lee, G. Matsunaga, T. Minami, S. Morita, S. Murakami, N. Nakajima, N. Nikai, S. Nishimura, I. Nomura, S. Ohdachi, K Ohkuni, M. Osakabe, R. Pavlichenko, B. Peterson, R. Sakamoto, H. Sanuki, M. Sasao, A. Shimizu, Y. Shirai, S. Sudo, S. Takagi, C Takahashi, S. Takayama, M. Takechi, K. Tanaka, K. Toi, K. Yamazaki, Y. Yoshimura and T. Watari,
Confinement Physics Study in a Small Low-Aspect-Ratio Helical Device CHS; Oct 1998
(IAEA-CN-69/OV4/5)

NIFS-569 M.M. Skoric, T. Sato, A. Maluckov, M.S. Jovanovic,
Micro- and Macro-scale Self-organization in a Dissipative Plasma; Oct. 1998

NIFS-570 T. Hayashi, N. Mizuguchi, T-H. Watanabe, T. Sato and the Complexity Simulation Group,
Nonlinear Simulations of Internal Reconnection Event in Spherical Tokamak; Oct. 1998
(IAEA-CN-69/TH3/3)

NIFS-571 A. Iiyoshi, A. Komori, A. Ejiri, M. Emoto, H. Funaba, M. Goto, K. Ida, H. Idei, S. Inagaki, S. Kado, O. Kaneko, K. Kawahata, S. Kubo, R. Kumazawa, S. Masuzaki, T. Minami, J. Miyazawa, T. Morisaki, S. Morita, S. Murakami, S. Muto, T. Muto, Y. Nagayama, Y. Nakamura, H. Nakanishi, K. Narihara, K. Nishimura, N. Noda, T. Kobuchi, S. Ohdachi, N. Ohyabu, Y. Oka, M. Osakabe, T. Ozaki, B.J. Peterson, A. Sagara, S. Sakakibara, R. Sakamoto, H. Sasao, M. Sasao, K. Sato, M. Sato, T. Seki, T. Shimozuma, M. Shoji, H. Suzuki, Y. Takeiri, K. Tanaka, K. Toi, T. Tokuzawa, K. Tsumori, I. Yamada, H. Yamada, S. Yamaguchi, M. Yokoyama, K.Y.Watanabe, T. Watari, R. Akiyama, H. Chikaraishi, K. Haba, S. Hamaguchi, S. Iima, S. Imagawa, N. Inoue, K. Iwamoto, S. Kitagawa, Y. Kubota, J. Kodaira, R. Maekawa, T. Mito. T. Nagasaka, A. Nishimura, Y. Takita, C. Takahashi, K. Takahata, K. Yamauchi, H. Tamura, T. Tsuzuki, S. Yamada, N. Yanagi, H. Yonezu, Y. Hamada, K. Matsuoka, K. Murai, K. Ohkubo, I. Ohtake, M. Okamoto, S. Sato, T. Satow, S. Sudo, S. Tanahashi, K. Yamazaki, M. Fujiwara and O. Motojima,
An Overview of the Large Helical Device Project; Oct. 1998
(IAEA-CN-69/OV1/4)

NIFS-572 M. Fujiwara, H. Yamada, A. Ejiri, M. Emoto, H. Funaba, M. Goto, K. Ida, H. Idei, S. Inagaki, S. Kado, O. Kaneko, K. Kawahata, A. Komori, S. Kubo, R. Kumazawa, S. Masuzaki, T. Minami, J. Miyazawa, T. Morisaki, S. Morita, S. Murakami, S. Muto, T. Muto, Y. Nagayama, Y. Nakamura, H. Nakanishi, K. Narihara, K. Nishimura, N. Noda, T. Kobuchi, S. Ohdachi, N. Ohyabu, Y. Oka, M. Osakabe, T. Ozaki, B. J. Peterson, A. Sagara, S. Sakakibara, R. Sakamoto, H. Sasao, M. Sasao, K. Sato, M. Sato, T. Seki, T. Shimozuma, M. Shoji, H. Sazuki, Y. Takeiri, K. Tanaka, K. Toi, T. Tokuzawa, K. Tsumori, I. Yamada, S. Yamaguchi, M. Yokoyama, K.Y. Watanabe, T. Watari, R. Akiyama, H. Chikaraishi, K. Haba, S. Hamaguchi, M. Iima, S. Imagawa, N. Inoue, K. Iwamoto, S. Kitagawa, Y. Kubota, J. Kodaira, R. Maekawa, T. Mito, T. Nagasaka, A. Nishimura, Y. Takita, C. Takahashi, K. Takahata, K. Yamauchi, H. Tamura, T. Tsuzuki, S. Yamada, N. Yanagi, H. Yonezu, Y. Hamada, K. Matsuoka, K. Murai, K. Ohkubo, I. Ohtake, M. Okamoto, S. Sato, T. Satow, S. Sudo, S. Tanahashi, K. Yamazaki, O. Motojima and A. Iiyoshi,
Plasma Confinement Studies in LHD; Oct. 1998
(IAEA-CN-69/EX2/3)

NIFS-573 O. Motojima, K. Akaishi, H. Chikaraishi, H. Funaba, S. Hamaguchi, S. Imagawa, S. Inagaki, N. Inoue, A. Iwamoto, S. Kitagawa, A. Komori, Y. Kubota, R. Maekawa, S. Masuzaki, T. Mito, J. Miyazawa, T. Morisaki, T. Muroga, T. Nagasaka, Y. Nakmura, A. Nishimura, K. Nishimura, N. Noda, N. Ohyabu, S. Sagara, S. Sakakibara, R. Sakamoto, S. Satoh, T. Satow, M. Shoji, H. Suzuki, K. Takahata, H. Tamura, K. Watanabe, H. Yamada, S. Yamada, S. Yamaguchi, K. Yamazaki, N. Yanagi, T. Baba, H. Hayashi, M. Iima, T. Inoue, S. Kato, T. Kato, T. Kondo, S. Moriuchi, H. Ogawa, I. Ohtake, K. Ooba, H. Sekiguchi, N. Suzuki, S. Takami, Y. Taniguchi, T. Tsuzuki, N. Yamamoto, K. Yasui, H. Yonezu, M. Fujiwara and A. Iiyoshi,
Progress Summary of LHD Engineering Design and Construction; Oct. 1998
(IAEA-CN-69/FT2/1)

NIFS-574 K. Toi, M. Takechi, S. Takagi, G. Matsunaga, M. Isobe, T. Kondo, M. Sasao, D.S. Darrow, K. Ohkuni, S. Ohdachi, R. Akiyama A. Fujisawa, M. Gotoh, H. Idei, K. Ida, H. Iguchi, S. Kado, M. Kojima, S. Kubo, S. Lee, K. Matsuoka, T. Minami, S. Morita, N. Nikai, S. Nishimura, S. Okamura, M. Osakabe, A. Shimizu, Y. Shirai, C. Takahashi, K. Tanaka, T. Watari and Y. Yoshimura,
Global MHD Modes Excited by Energetic Ions in Heliotron/Torsatron Plasmas; Oct. 1998
(IAEA-CN-69/EXP1/19)

NIFS-575 Y. Hamada, A. Nishizawa, Y. Kawasumi, A. Fujisawa, M. Kojima, K. Narihara, K. Ida, A. Ejiri, S. Ohdachi, K. Kawahata, K. Toi, K. Sato, T. Seki, H. Iguchi, K. Adachi, S. Hidekuma, S.Hirokura, K. Iwasaki, T. Ido, R. Kumazawa, H. Kuramoto, T. Minami, I.. Nomura, M. Sasao, K.N. Sato, T. Tsuzuki, I. Yamada and T. Watari,
Potential Turbulence in Tokamak Plasmas; Oct. 1998
(IAEA-CN-69/EXP2/14)

NIFS-576 S. Murakami, U. Gasparino, H. Idei, S. Kubo, H. Maassberg, N. Marushchenko, N. Nakajima, M. Romé and M. Okamoto,
5D Simulation Study of Suprathermal Electron Transport in Non-Axisymmetric Plasmas; Oct. 1998
(IAEA-CN-69/THP1/01)

NIFS-577 S. Fujiwara and T. Sato,
Molecular Dynamics Simulation of Structure Formation of Short Chain Molecules; Nov. 1998

NIFS-578 T. Yamagishi,
Eigenfunctions for Vlasov Equation in Multi-species Plasmas Nov. 1998

NIFS-579 M. Tanaka, A. Yu Grosberg and T. Tanaka,
Molecular Dynamics of Strongly-Coupled Multichain Coulomb Polymers in Pure and Salt Aqueous Solutions; Nov. 1998

NIFS-580 J. Chen, N. Nakajima and M. Okamoto,
Global Mode Analysis of Ideal MHD Modes in a Heliotron/Torsatron System: I. Mercier-unstable Equilibria; Dec. 1998

NIFS-581 M. Tanaka, A. Yu Grosberg and T. Tanaka,
Comparison of Multichain Coulomb Polymers in Isolated and Periodic Systems: Molecular Dynamics Study; Jan. 1999